

Supporting information:

Porphyrin-palladium hydride MOF nanoparticles for tumor-targeted photoacoustic imaging-guided hydrogenothermal therapy of cancer

*Gaoxin Zhou,^a Yingshuai Wang,^a Zhaokui Jin,^a Penghe Zhao,^a Han Zhang,^b Yanyuan Wen,^a
Qianjun He^{*a}*

^a Guangdong Provincial Key Laboratory of Biomedical Measurements and Ultrasound Imaging, National-Regional Key Technology Engineering Laboratory for Medical Ultrasound, School of Biomedical Engineering, Health Science Center, Shenzhen University, No. 1066 Xueyuan Road, Nanshan District, Shenzhen 518060, Guangdong, China

^b Key Laboratory of Optoelectronic Devices and Systems of Ministry of Education and Guangdong Province, College of optoelectronic Engineering, Shenzhen University, Shenzhen 518060, Guangdong, China

Corresponding Author: E-mail: nanoflower@126.com

Experimental section.

Chemicals and reagents. Sodium tetrachloropalladate (II) (Na_2PdCl_4), 5,10,15,20-tetrakis(4-pyridyl)-21H,23H-porphine (TPyP) and hydrazine were purchased from J&K Scientific Ltd (Beijing, China). Polyvinylpyrrolidone (PVP, $M_w=55000$) and hydrochloric acid (37%) were provided by Sinopharm Chemical Reagent Co., Ltd. Cell Counting Kit-8 (CCK-8), DAPI and calcein-AM/PI were obtained from Beyotime Biotechnology Co., Ltd. Pure water ($18.2 \text{ M}\Omega\cdot\text{cm}$) used in the experiments was produced from a Milli-Q Academic system (Millipore Corp., Billerica, MA, USA). Two cancer cell, human cervical carcinoma HeLa cell and mouse breast cancer 4T1 cell, one normal cell, human breast epithelial MCF10A cell were provided by Cell Bank of Shanghai Institute of Cell Biology, Chinese Academy of Sciences.

Characterization. The high-angle annular dark-field (HAADF) and energy dispersive X-ray spectroscopy elemental mapping images were obtained on a field emission JEM-2100F microscope (JEOL, Japan). Scan electron microscopy (SEM) images observed by Ultra Plus scanning electron microscopy (Zeiss, Germany). X-ray diffraction (XRD) of PdCl_2 -MOF nanoparticles were conducted using a UltimaIV (Rigaku, Japan) diffractometer ($\text{Cu K}\alpha$, $\lambda = 1.54056 \text{ \AA}$) operated at 40 kV and 200 mA on the Si substrate. The experimental diffraction patterns were collected with scanning range (2θ) of $5\text{--}80^\circ$ and step interval of 0.02° on a Si substrate. X-ray photoelectron spectroscopy (XPS) measurements were performed on a K-Alpha+ X-ray photoelectron spectrometer with a monochromatic Al $\text{K}\alpha$ X-ray source (Thermo Scientific, USA). Fourier transform infrared (FT-IR) spectroscopy were acquired using a Spectrum II spectrophotometer (PerkinElmer, USA) in the region $4000\text{--}400 \text{ cm}^{-1}$ with a KBr pellet. Thermal Gravity Analyses (TGA) was carried out with a TGA

Q50 (TA instrument, USA) at a scanning rate of 5 °C min⁻¹. Air was used as the sample gas for the TG measurements at a flow rate of 20 mL min⁻¹ and the temperature range was from 25 °C to 800 °C. Dynamic light scattering (DLS) measurement was conducted on a Nano-ZS 90 Nanosizer (Malvern, UK). UV-VIS-NIR absorption spectra were measured using a Cary 60 spectrofluorometer (Agilent, USA). Fluorescence spectra were recorded on a Lumina spectrofluorometer (Thermo Scientific, USA).

Preparation of PdH-Porphyrin metal-organic framework nanomedicine. Firstly, TPyP (20 mg, 0.032 mmol) was dissolved with 10 mL of 0.01 M hydrochloric acid, Na₂PdCl₄ (19 mg, 0.064 mmol) was dissolved with 10 mL of pure water, TPyP solution was quickly added into Na₂PdCl₄ solution under vigorously stirring. After 30 min 10 mg of PVP was added to the suspension and the reaction accomplished after 4 h, the suspension was centrifuged at 12000 rpm for 20 min, the obtained nanoparticles were washed with pure water for three times and redispersed in water.

To obtain zero-valence palladium contained MOF, the suspension of PdCl₂-MOF was reduced by hydrazine. Typically, 10 mL of PdCl₂-MOF (10 mg) suspension was sonicated for 10 min using a water-bath sonicator, then 10 μL of hydrazine was added into the solution with intensively stirring. After 8 h, the particle product was collected by centrifuge and washed 3 times with pure water, the collected Pd-MOF nanoparticles were redispersed into water.

To load hydrogen, the Pd-MOF solution was bubbled with hydrogen gas for 30 min at a relatively slow gas flow rate under stirring. The resulting solution contained the final product PdH-MOF nanoparticles.

Measurement of the release of reductive hydrogen from the PdH-MOF nanoparticles using MB probe method. MB can be reduced to colorless reduced MB (leucomethylene blue, leucoMB) by hydrogen gas in the presence of catalyst such as platinum or palladium. Based on this principle, MB-Pt reagent usually was served as a probe for determination of hydrogen concentration in water by titration method. We found that zero-valent Pd in Pd-MOF nanoparticles have similar catalytic hydrogenation effect as Pt, so a UV-VIS spectrum method for *in situ* quantitative detection of hydrogen release from PdH-MOF nanoparticles was established. Because of the linear relation between absorbance of MB at 664 nm and the concentration of hydrogen, the release of reductive hydrogen from PdH-MOF can be monitored by real-time detection of the absorbance of MB using UV-VIS spectrometer. The specific measurement steps are described as follows: Firstly, a 1-cm quartz cuvette was filled with 3.4 mL MB solution (15 μM), the solution was bubbled with nitrogen for 30 min to decimate the dissolved oxygen, then the PdH-MOF solution (0.1 mL) was gently added and the cuvette was sealed tightly, from this point on, the absorbance of MB was monitored at specific time intervals, until the absorbance at 664 nm keep a constant. It is noticeable that the concentration of MB should not exceed the linearity range of UV-VIS, and should also be high enough to completely react with released hydrogen from PdH-MOF nanoparticles. A linear standard curve of absorbance vs concentration of MB at 664 nm wavelength over the range up to 8 $\mu\text{g mL}^{-1}$ was plotted. The concentration of reductive hydrogen concentration released was calculated from the final absorbance of MB and the formula of standard curve.

Establishment of mouse breast cancer model. All the animals in this study received humane care in compliance with the institution's guidelines for the maintenance and use of laboratory animals in research. Animal procedures involving animals in this

study were in accordance with ethical standards and approved by the Institutional Animal Care and Use Committee of Shenzhen University. Female BALB/c mice aged 4 weeks (weighted 18~22 g) were obtained from Guangdong Medical Laboratory Animal Center (Guangzhou, China). After accommodated for 1 week in animal room, all rats were injected with mouse breast cancer 4T1 cells (100 μ L, 3×10^6) subcutaneously into the right hind legs. After 7~10 days, mouse cancer model was successfully established when the volume of tumor reached to $\sim 100 \text{ mm}^3$.

Photothermal performance and *in vivo* photothermal imaging of Pd-MOF and PdH-MOF. Photothermal heating curves of nanoparticles were plotted by monitoring the temperature change with time of samples solution in Eppendorf tubes under the irradiation of 808 nm NIR laser at different power densities (0.2, 0.5, 1.0 W cm^{-2} , KS-810F-8000, Kai Site Electronic Technology Co., Ltd.). The temperatures were recorded by a fixed-mounted thermal imaging camera (FLIR A300-series). The photothermal conversion efficacies (η) of Pd-MOF and PdH-MOF nanoparticles were calculated according to Roper's method as following.^[1]

$$\eta = \frac{hA(T_{max} - T_{amb}) - Q_0}{I(1 - 10^{-A_\lambda})} \quad (1)$$

Where Q_0 was measured independently using water without nanoparticles. T_{max} is the highest temperature reached after laser irradiation, T_{amb} is the ambient temperature, I is the input laser power, A_λ is the absorbance of nanoparticles at 808 nm. Further, hA is determined based on a dimensionless driving force temperature θ , and τ_s is a sample system constant.

$$\theta = \frac{T - T_{amb}}{T_{max} - T_{amb}} \quad (2)$$

$$\tau_s = \frac{\sum_i m_i C_{p,i}}{hA} \quad (3)$$

$$t = -\tau_s \ln \theta \quad (4)$$

τ_s equals to the slope of linear equation that is obtained from simulation of linearity curve of time data (t) versus $-\ln \theta$ during cooling period. The m_i and $C_{p,i}$ are the mass and heat capacities of water, respectively. Then hA can be obtained from equation 3 and used to calculate η using equation 1.

For *in vivo* photothermal imaging, tumor-bearing mice were intravenously injected with nanoparticles in veil, after 4 h, the near infrared images of whole body were taken under the irradiation of 808 nm NIR laser (1 W cm^{-2}) under 4% chloral hydrate anesthesia. Control experiment using PBS was conducted following the same process to evaluate the intratumoral retention efficiency of nanoparticles.

***In vitro* and *in vivo* PAI.** PAI *in vitro* and *in vivo* were all accomplished by a Vevo 2100 LAZR system with the following parameter: excitation wavelength: 700 nm, PA gain: 28 dB. To evaluate the quantitative relationship between the PA signal and PdH-MOF concentration, PdH-MOF solutions with concentration between 20~320 $\mu\text{g mL}^{-1}$ were added into Eppendorf tubes and immersed into water to detect their PA signals. For *in vivo* PAI study, when the tumor size reached $\sim 200 \text{ mm}^3$, mice were anesthetized by 1.5% isoflurane delivered via a nose cone and PAI were taken before and after the intravenous injection of aqueous suspension of PdH-MOF at a dose of 10 mg kg^{-1} body weight. It is noticeable that mice' hair around tumor was carefully

removed with surgical clipper and depilatory to avoid noise and acquire high-quality images.

Biodistribution of PdH-MOF by fluorescence imaging. To investigate the accumulation and metabolism behavior of PdH-MOF nanoparticles in tumor and major organ tissues in mice, fluorescence imaging was conducted. 4T1 tumor-bearing mice were intravenously injected PdCl₂-MOF nanoparticle (10 mg kg⁻¹ body weight, PdCl₂-MOF have the same size and main components except for stronger fluorescence property was injected instead of PdH-MOF), after 8 h the mice were euthanized and dissected, tumor, heart, liver, spleen, lung and kidney were collected and rinsed with water. The fluorescence images were taken using an IVIS Lumina II +XGI-8 (Caliper Life Science, USA) real-time *in vivo* near infrared fluorescence imaging system (excitation filter: 605 nm; emission filter: Cy5.5).

Confocal Fluorescence Imaging. HeLa cells were seeded into a CLSM dish and cultured in 2 mL of DMEM containing 10% FBS at 37 °C under 5% CO₂ atmosphere. After incubation for 12 h, the culture medium was replaced with fresh ones containing Pd-MOF and PdH-MOF nanoparticles (200 µg mL⁻¹) and maintained for another 3 h, then the dishes were divided into two groups, with or without a 808 nm laser irradiation at a power density of 1 W cm⁻² for 10 min respectively. After incubation for 8 h, the culture medium in all dishes were discarded and the dishes were washed with PBS for 2 times, calcein-AM/PI double staining kit was used to stain living and dead cells respectively. PBS group with or without laser irradiation were served as control. The stained cells were observed as soon as quickly using a Leica TCS SP5 II (Germany) CLSM microscope with 488/515 nm (calcein-AM) and 543/594 nm (PI) as excitation/emission wavelength.

***In vitro* photothermal and hydrogen combined therapy.** CCK-8 assays were conducted using HeLa and 4T1 cells to evaluate the therapeutic efficacy of nanomedicine combined with photothermal effect. The experiment was divided into six groups: (1) PBS control, (2) PBS+laser, (3) Pd-MOF, (4) Pd-MOF+laser, (5) PdH-MOF, (6) PdH-MOF+laser. The cells were seeded in 96-well plates at cell density of 1×10^4 cells/well for 24 h at 37 °C. Afterwards, the culture medium was refreshed by 100 μ L nanoparticle containing DMEM with 10% FBS. The concentration of Pd-MOF and PdH-MOF nanoparticles were in the range of 0~200 μ g mL⁻¹. After 3 h incubation, cells of the photothermal therapy group (2, 4, 6) were irradiated by a 808 nm laser at two power intensity: 0.5 and 1.0 W cm⁻² respectively. After irradiation treatment the cells were incubated to 24 h, then each well was added with 10 μ L of CCK-8 agent and kept at 37 °C for 1 h, the OD value at 450 nm was measured using a Synergy H1 (Biotek, USA) microplate spectrophotometer. The cell viability was calculated from OD value in each well by comparison with blank control. Each data point was represented as a mean \pm standard deviation of five independent experiments ($n = 5$). The same procedure without laser irradiation was performed using MCF10A cell to assessment the toxicity of nanomedicine to normal cells.

***In vivo* photothermal and hydrogenothermal combined therapy.** The 4T1 tumor-bearing mice were randomly divided into six groups when the tumor size reached ~ 100 mm³. (1) PBS control, (2) PBS+laser, (3) Pd-MOF, (4) Pd-MOF+laser, (5) PdH-MOF, (6) PdH-MOF+laser ($n=5$). Mice were intravenously injected with 100 μ L of 0.01 M PBS for group (1) and (2), 10 mg kg⁻¹ body weight Pd-MOF nanoparticles for group (3) and (4), 10 mg kg⁻¹ body weight PdH-MOF nanoparticles for group (5) and (6). After intravenously injection for 1 h, the mice in group (2), (4), (6) were irradiated by a 808 nm laser at the power density of 0.5 W cm⁻² for 10 min. After

treatments, the tumor volumes were measured by a vernier caliper every day for 17 days and calculated according to the following formula: $\text{Length} \times \text{Wide} \times \text{Wide} / 2$. Body weight of each mouse was also recorded every 2 days. Mice were euthanized on day 17 and the tumors were weighted. To appraise the *in vivo* biocompatibility of Pd-MOF and PdH-MOF nanoparticles, major organs such as heart, liver, spleen, lung and kidney were excised and resected, then fixed in a 4% polyoxymethylene solution and embedded in paraffin for hematoxylin and eosin (H&E) staining.

The hemotoxicity and liver/kidney function analyses. Two weeks old BALB/c mice were randomly divided into 5 groups ($n = 4$ per group), which were intravenously injected with 100 μL PBS (as control), PdH-MOF nanoparticles were injected at different dosage of 10, 20, 50, 100 mg kg^{-1} body weight and further feeding for two weeks. Then the blood of each mouse was collected and detected by blood cell analyzer (BC-31S, Mindray) and biochemical analyzer (iMagic-M7, Icubeo).

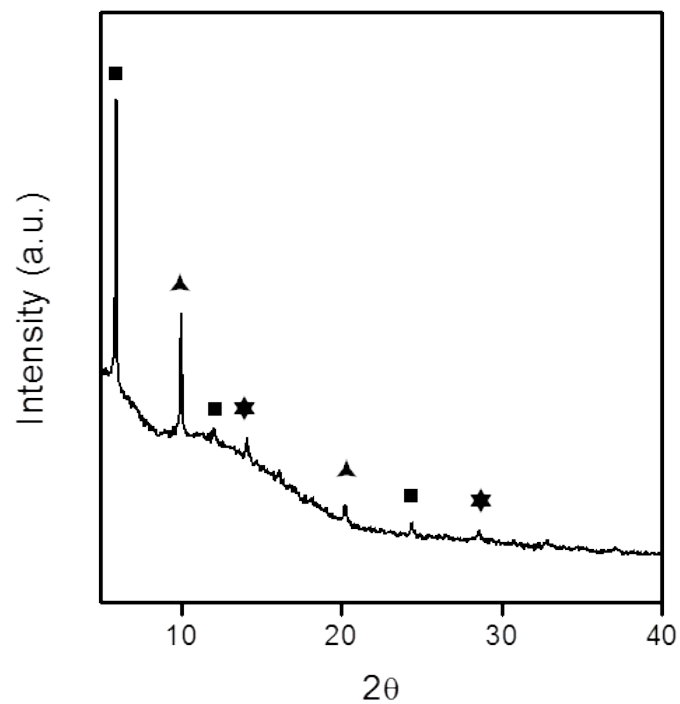


Figure S1. XRD spectrum for the PdCl₂-MOF nanoparticles.

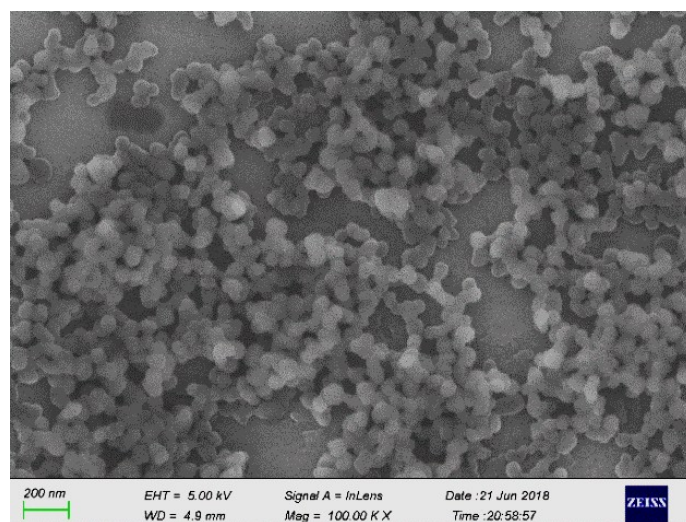


Figure S2. SEM image of PdCl₂-MOF nanoparticles.

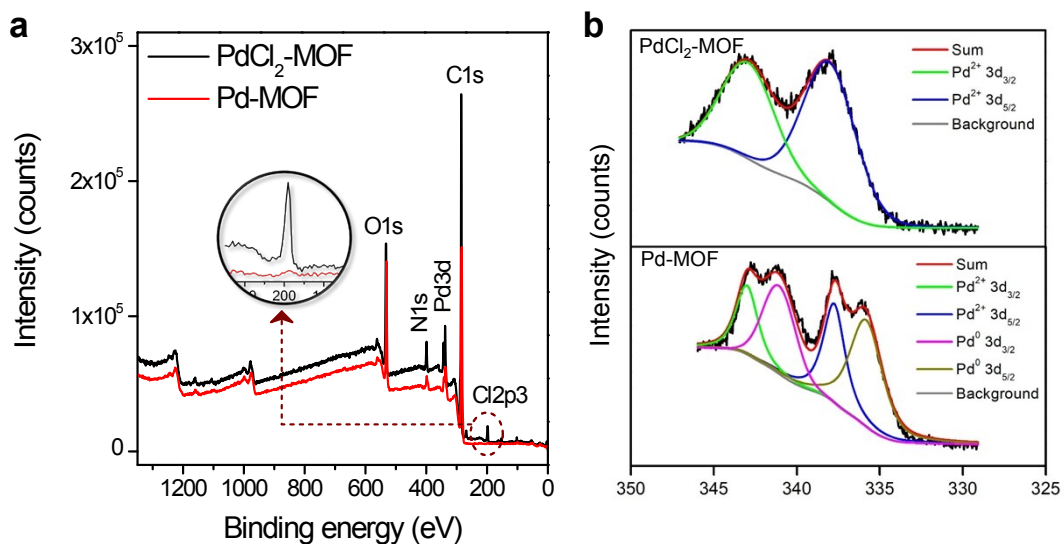


Figure S3. XPS (a) total and (b) high resolution Pd3d curves of porphyrin-palladium MOF nanoparticles.

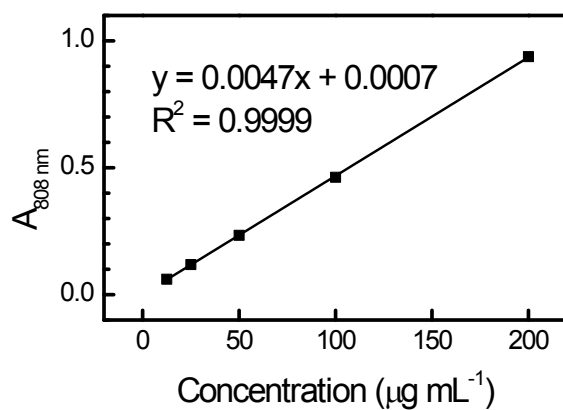


Figure. S4. Relationship between absorbance intensity at 808 nm and Pd-MOF concentration.

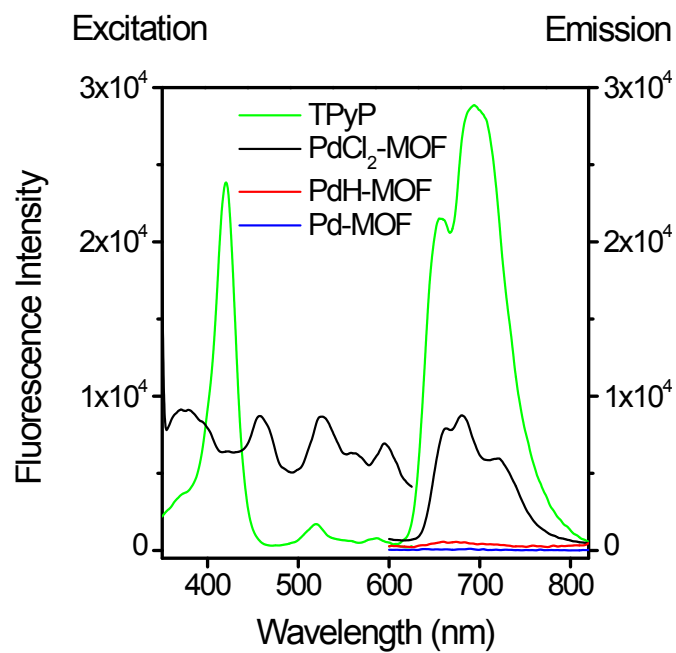


Figure S5. The fluorescence excitation and emission spectra of free TPyP hydrochloric solution and aqueous dispersion of PdCl₂-MOF, Pd-MOF and PdH-MOF. Excitation wavelength: 425 nm, emission wavelength: 660 nm.

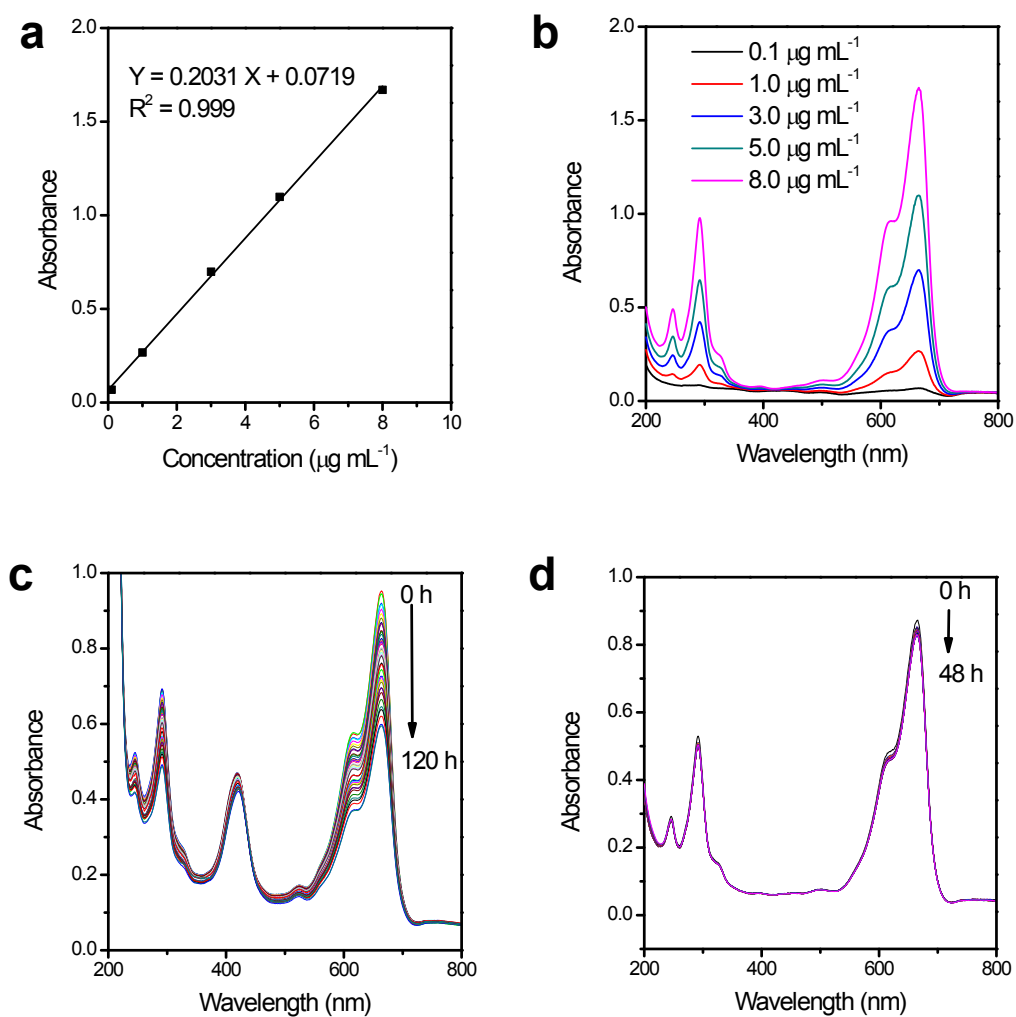


Figure S6. The UV-VIS-NIR absorption spectra of methylene blue (MB). (a) The standard curve of MB linearly fitted between absorbance at 664 nm and concentration of MB standard solutions. $Y = 0.2031 X + 0.0719$, $R^2 = 0.999$. (b) The UV-VIS absorption spectra of MB standard solution at concentration of 0.1, 1, 3, 5 and 8 $\mu\text{g mL}^{-1}$. (c) The time-dependent change of UV-VIS absorption spectra of MB after addition of PdH-MOF nanoparticles from 0 h to 120 h. (d) The time-dependent change of UV-VIS absorption spectra of MB after it was added to hydrogen gas saturated water from 0 h to 48 h.

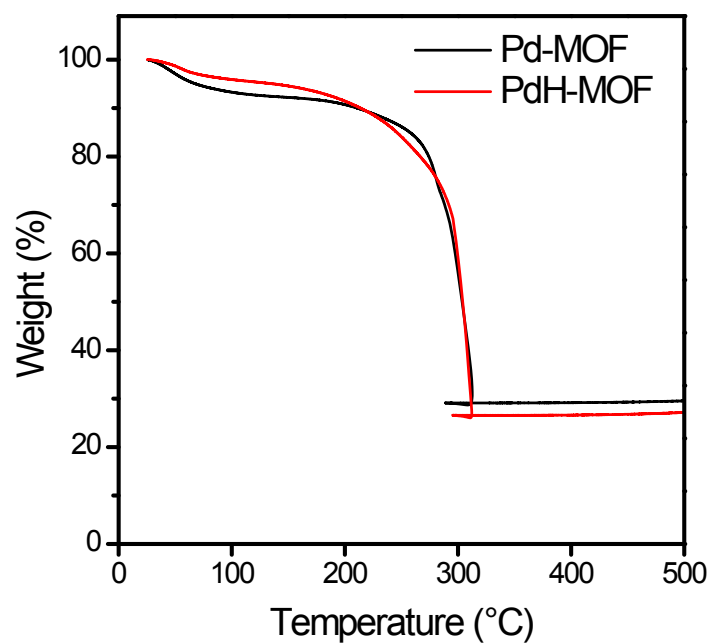


Figure S7. TGA curves of Pd-MOF and PdH-MOF nanoparticles.

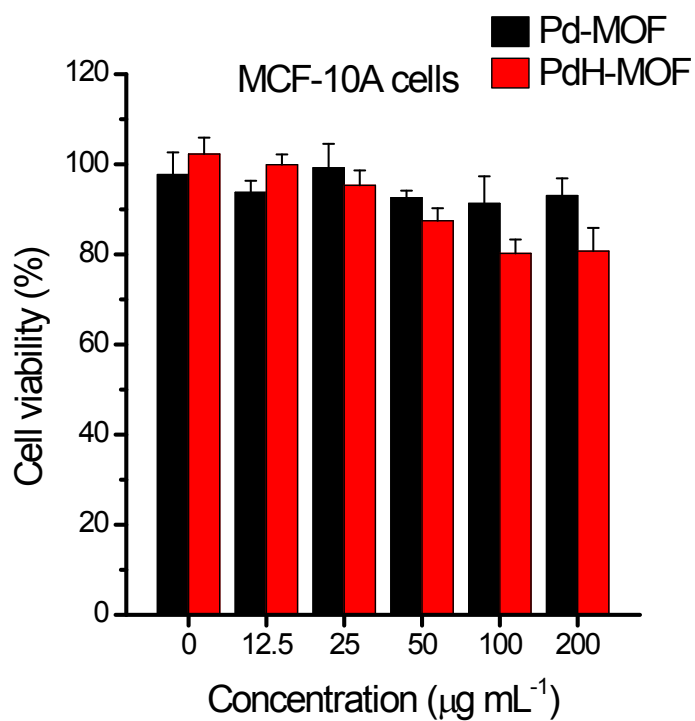


Figure S8. Cell viability of normal MCF-10A cells at 24 h after treatment with aqueous dispersion of Pd-MOF and PdH-MOF.

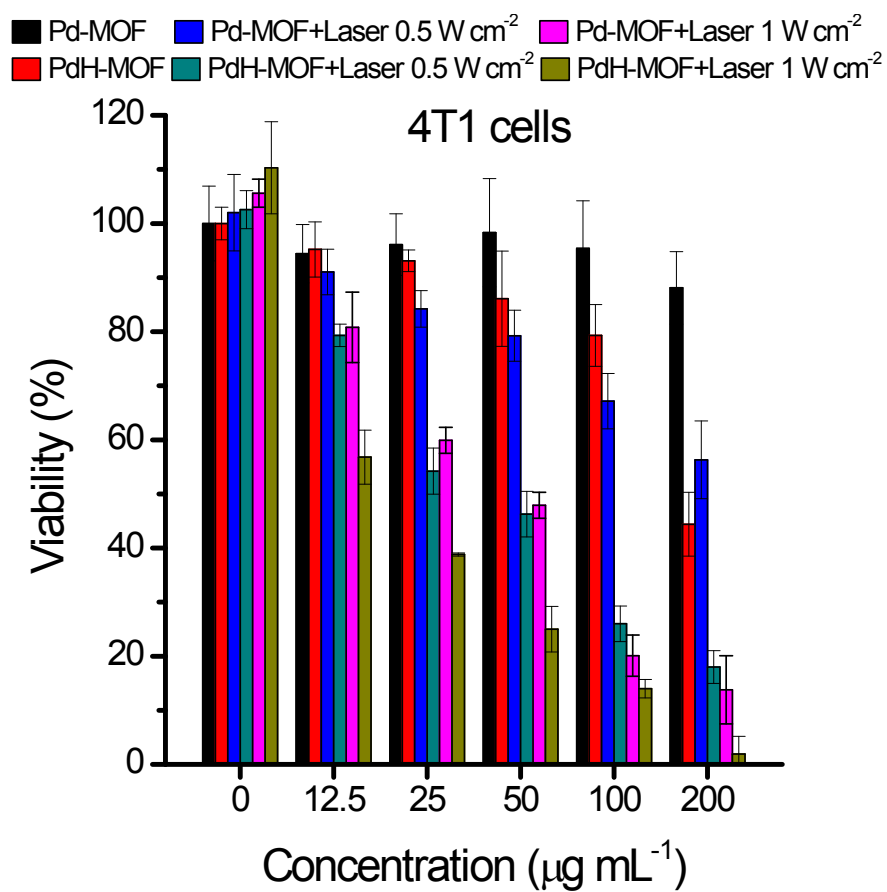


Figure S9. Cell viability of 4T1 cells treated with different concentrations of nanoparticles for 24 h with or without 808 nm laser irradiation (10 min, 0.5, 1 W cm^{-2}).

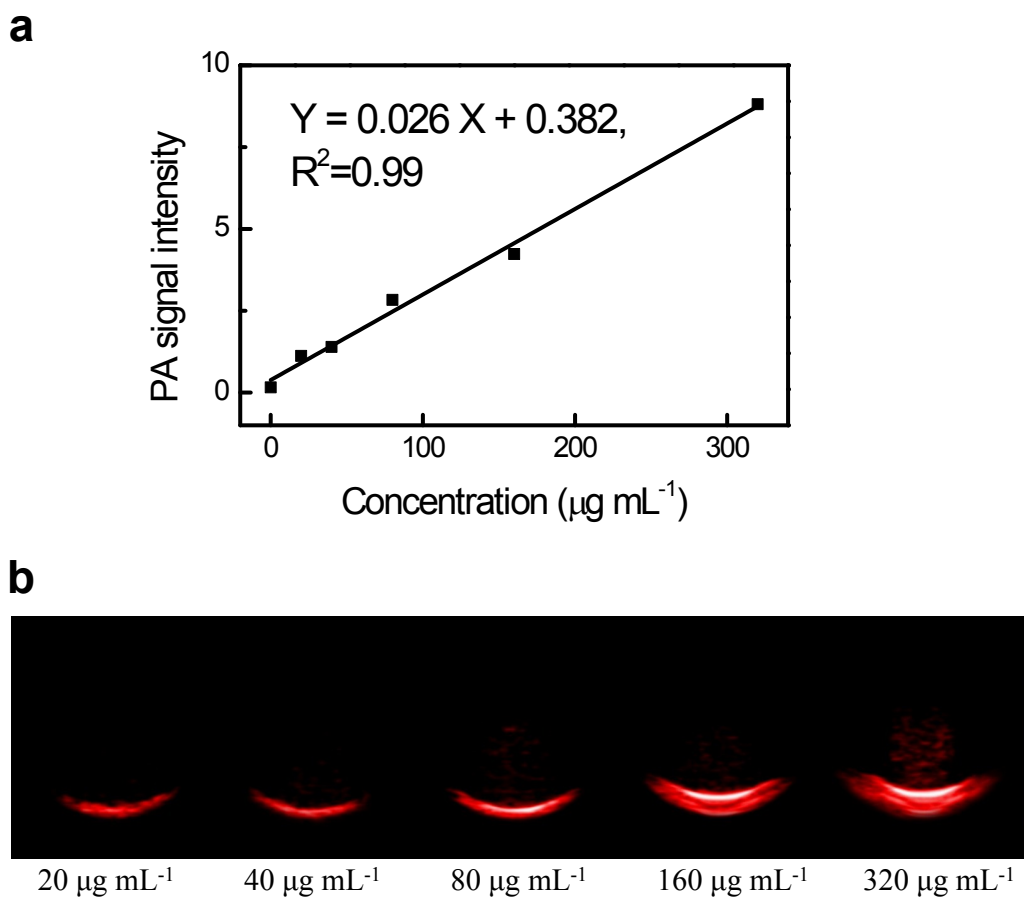


Figure S10. *In vitro* PAI. (a) The linearly fitted standard curve of PA signal vs concentration of aqueous suspension of PdH-MOF nanoparticles. $Y = 0.026 X + 0.382$, $R^2 = 0.99$. (b) The dependence of PA imaging signal of aqueous suspension of PdH-MOF nanoparticles on its concentration (20, 40, 80, 160 and 320 $\mu\text{g mL}^{-1}$).

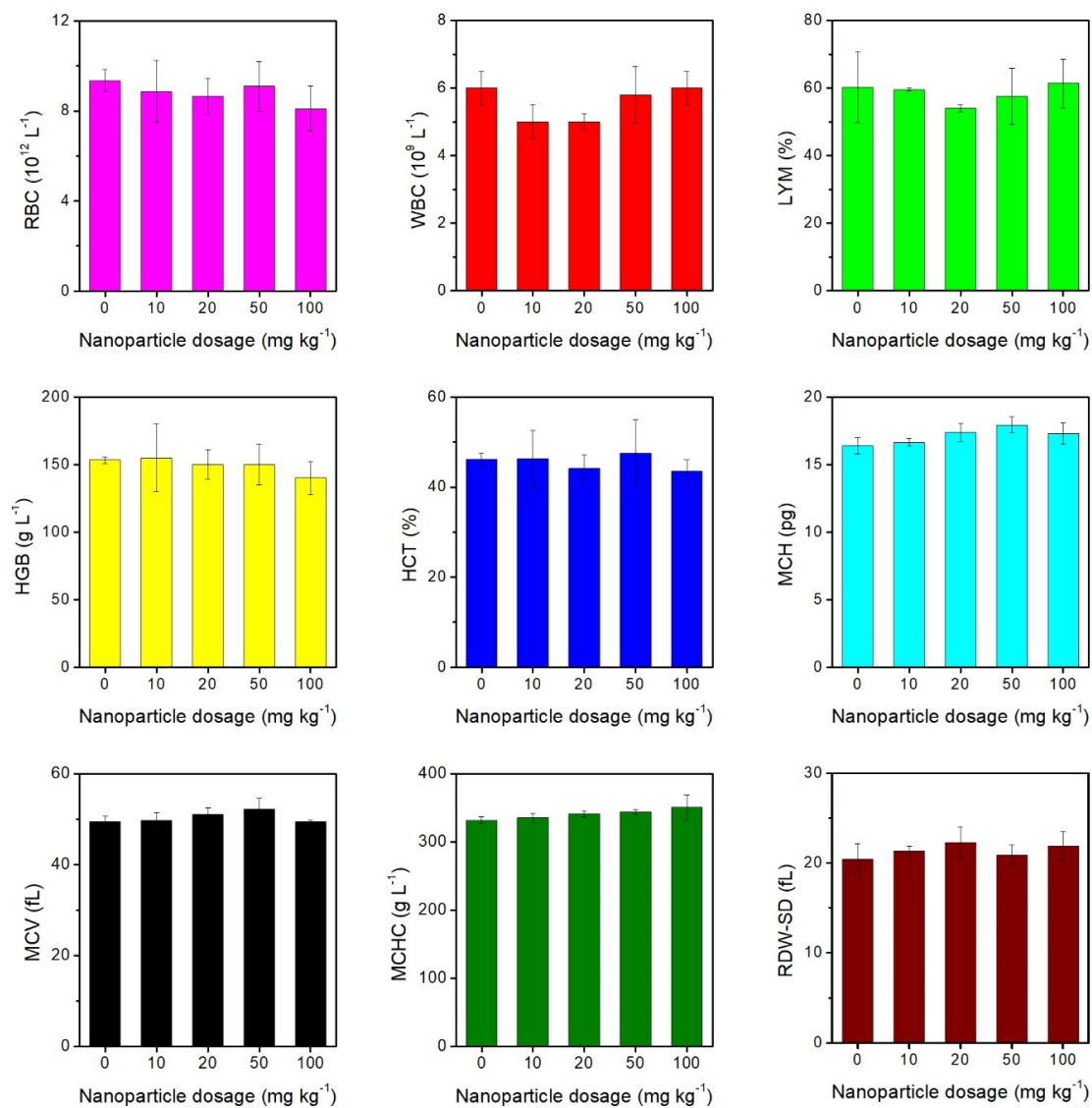


Figure S11. The evaluation of standard haematology markers including RBC, WBC, LYM, HGB, HCT, MCH, MCV, MCHC and RDW-SD. Mice were intravenously injected with PdH-MOF nanoparticles at different dosage of 10, 20, 50, 100 mg kg⁻¹ body weight, and further feeding for two weeks.

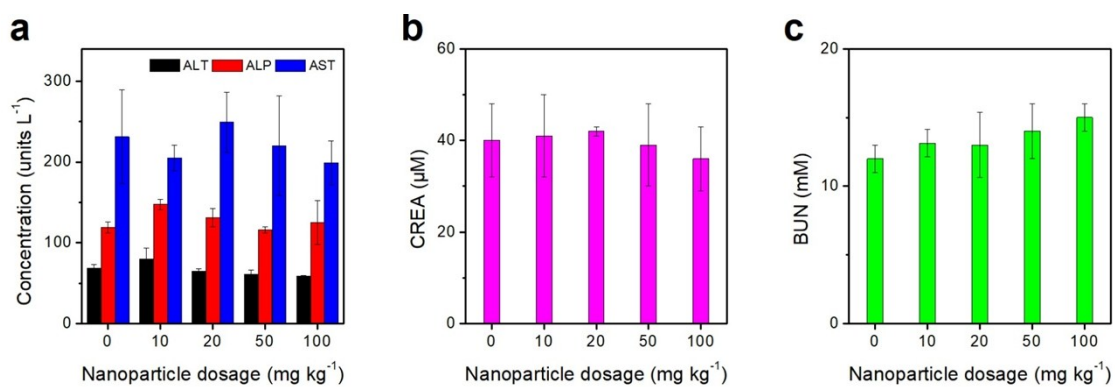


Figure S12. Blood biochemical analyses including liver functions (a) and kidney functions (b,c). Mice were grouped and treated as in haematology assay.

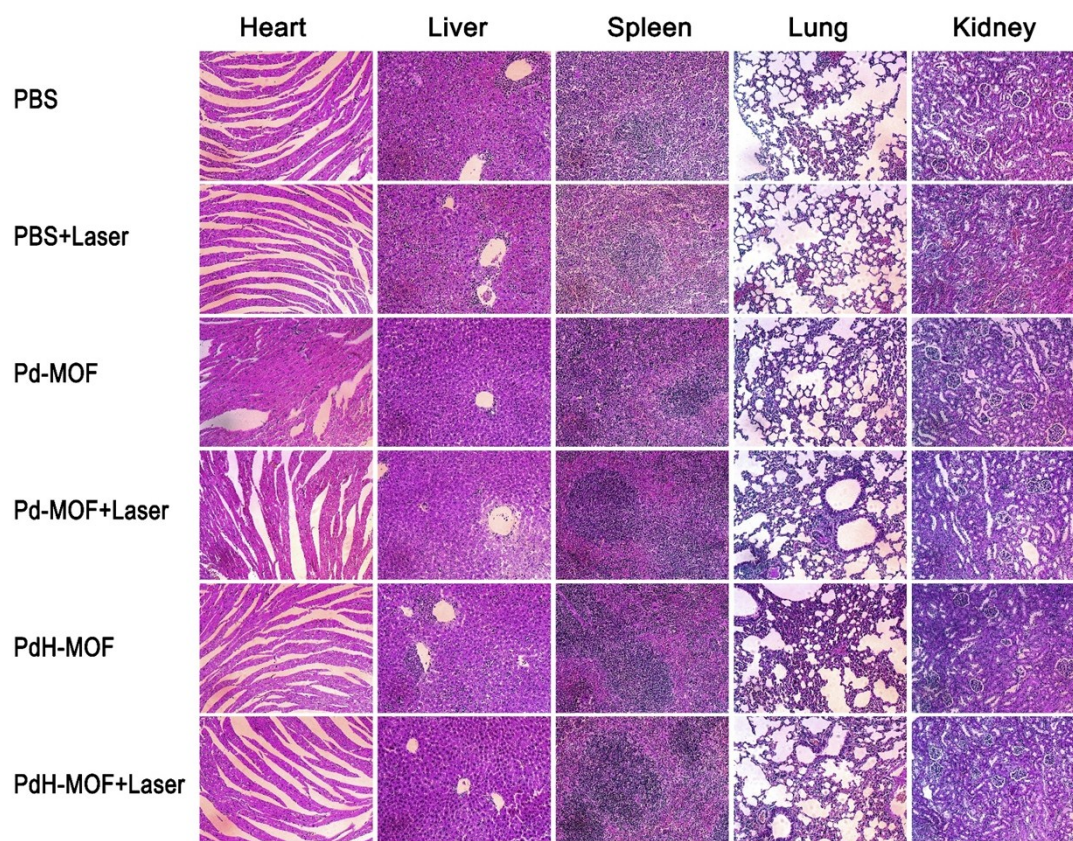


Figure S13. H&E-stained tissue sections of major organs, including the heart, liver, spleen, lung, and kidney from mice in different treatment groups.

References

1. D. K. Roper, W. Ahn, M. Hoepfner, *J. Phys. Chem. C* 2007, **111**, 3636–3641.